The International Journal of Advanced Manufacturing Technology (2019) 100:1881–1892
https://doi.org/10.1007/s00170-018-2794-z

ORIGINAL ARTICLE

Effect of cutter body geometry in Ti-6Al-4V face-milling process

Ning Li[1] · Yongjie Chen[1] · Dongdong Kong[1]

Received: 28 February 2018 / Accepted: 28 September 2018 / Published online: 11 October 2018

Abstract
Tool geometry has a direct impact on workpiece deformation, cutting forces, and tool wear, thereby affecting machinability, surface quality, and tool life. However, the research about the effect of cutter body geometry on cutting performance has rarely been reported. In this paper, the performance of the same series of indexable face-milling cutters with different diameters was investigated. The dynamic characteristic analysis results show that the cutter with diameter of 80 mm is the least susceptible to resonance due to the highest first-order modal frequency of 13,201 Hz. The cutter body geometry has a significant impact on mode shapes. The cutting performance tests show that the milling cutter with a diameter of 125 mm performs the best in terms of static force and maximum dynamic force in the *Z* direction and wear resistance. In view of the overall situation, the machined surface quality of the cutter with a diameter of 40 mm is the worst, whose abnormalities can be attributed to the vibration caused by the change of cutting depth and the formation and abscission of built-up edge. By the analysis of geometric structure, the center offset and the installation angle of indexable insert, together with the outline dimensions of the cutter body, jointly determine the tool cutting performance. The present work will provide guidance for the design of indexable milling cutters for high-performance machining of titanium alloys.

Keywords Ti-6Al-4V · Dynamic characteristic · Static force · Maximum dynamic force · Surface roughness · Tool wear rate

1 Introduction

Improving machining efficiency is a constant pursuit of a cutting process, and it is also one of the driving forces for continuous improvement of cutting technology. High-speed milling is a main research direction due to the advantages of high flexibility, high material-removal rate, and multiple edges engaged in cutting simultaneously. Currently, it has been extensively used in the automotive, aerospace, and molds/dies industries to reduce processing time and/or eliminate post-processing like polishing [1]. However, the increase in cutting speed will accelerate tool wear and even lead to rapid failure of the cutting edges, which in turn increases production costs. To this end, many researches have been carried out in recent years to improve the cutting performance of tools.

The material, geometry, and structure of the tool engaged in cutting are the three major factors that determine the cutting performance. Among them, the tool material plays a key role, which has a great influence on tool life, machining efficiency, machining quality, and machining cost [2]. The continuous development of modern cutting technology toward high efficiency, high accuracy, and automation puts forward new requirements for cutting tools. For this sake, in the early 1950s, the cemented carbide indexable tool was successfully developed, which was a major breakthrough in the history of tool development. Since then, it has been widely used in automatic production lines due to its advantages such as quick tool changing, accurate positioning, high efficiency, easy to use, and low comprehensive cost [3]. At the same time, high development and widespread use of modern powder metallurgy technology, CNC grinding technology, and CAD/CAM tool technology open up vast possibilities for the design, modeling, and manufacture of carbide indexable inserts, which are generally fabricated by pressing into optimized shapes. To be sure, any insert with a complex shape can be made by pressing process, which means the maturity of indexable insert manufacturing technology.

A study published by CIRP in 1969 pointed out that the allowable cutting speed of cutting tools could be doubled due to the improvement of tool material [4]. Therefore, many advanced materials and new coatings have been developed to

✉ Ning Li
lining19880701@163.com

[1] School of Mechanical Science and Engineering, Huazhong University of Science and Technology, Wuhan 430074, China

improve cutting performance. Han et al. [5] designed and fabricated a novel indexable TiC-Ni cermet tool toughened by TiN nanoparticles, which was used for face milling of AISI 1045. The results proved that it had an advantage of high-speed cutting performance. Kim et al. [6] investigated the relationship between microstructure, mechanical properties, and micro end-milling performance of various Ti-based solid solution cermets and found that excellent fracture toughness and reasonable hardness were the primary reasons for improving tool performance. Due to the excellent impact toughness, crush resistance, and high-temperature resistance, PCD and PCBN tools were utilized by Su et al. [7] in high-speed milling of TA15, and their performance and wear mechanisms were investigated. Ogawa et al. [8] carried out a study on the mass production of binder-less PCD micro-milling tools using femtosecond pulsed lasers due to its extremely high performance for machining nonferrous materials. Lu et al. [9] investigated the effect of CrTiAlN hard coating composed of Cr adhesive layer, CrN interlayer, and CrTiAlN top layer on the cutting performance of the cemented carbide-end mills. By comparison with the uncoated-end mills, the coated ones showed significant improvement on tool life and a much lower cutting force. In order to solve the problem of poor adhesion of diamond coatings, SiC interlayers were pre-produced on cemented carbide micro-end mills by Hei et al. [10] for the subsequent deposition of diamond coatings. The results showed that these bilayer-coated tools exhibited better cutting performance than the uncoated tools. Skordaris et al. [11] investigated the effect of film thickness on mechanical properties and milling performance of nano-structured multi-layer PVD-coated cemented carbide tools and found that tool life was prolonged almost proportionally with the coating thickness augmentation. Aslantas et al. [12] found that the cutting performance of NCD-coated tools was lower than that of TiN- and AlCrN-coated tools during micro-milling of Ti-6Al-4V. Liu et al. [13] systematically investigated the effects of gas pressure on microstructure, deposition rate, coating thickness, phase constitution, mechanical properties, cutting performance, and wear mechanism of (Ti, Al, Zr) N coatings on the Si_3N_4 ceramic tools, and found that the coated tools produced at a gas pressure of 2.5 Pa exhibited the best performance. Afterwards, they deposited CrAlN and TiAlN coatings on the Si_3N_4 ceramic inserts by PVD process-cathodic arc evaporation method, and found that these coatings could protect the insert substrates effectively, and the CrAlN coated inserts showed the best machining quality [14]. Although some achievements have been made, the development of new materials or coatings needs more time and a higher cost.

Simultaneously, CIRP also pointed out that every other decade, tool durability could be almost two times higher due to improved tool structure and optimized process parameters [4]. Furthermore, productivity can also be significantly improved. Based on this, many researches have been conducted. Saptaji et al. [15] experimentally investigated the effect of side wall edge strengthening on top burr formation during micro-milling slots of Al-6061 alloy with a carbide tool, and found that top burrs were reduced when changing work surface geometry or introducing a taper in the micro-milling tool. Subramanian et al. [16] focused on the influence of radial rake angle, nose radius, feed rate, and axial depth of cut on vibration amplitude, and found that the vibration amplitude was negatively correlated with radial rake angle and nose radius. Ji et al. [17] investigated the effects of the geometric parameter of face-milling cutters such as number of cutter teeth, gullet shape, and volume on the generation of aerodynamic noise so as to depress the overall aerodynamic noise. Huang et al. [18] investigated the machinability of variable pitch tools during milling of aeronautical thin-wall material Ti-6Al-4 V, and found that the vibration was obviously decreased when compared with uniform pitch tool. Warhanek et al. [19] conducted an experimental study on the influence of tool geometry on cutting characteristics and tool wear during milling of sintered zirconia dioxide to examine the applicability. Zhu et al. [20] investigated the effects of cutting parameters and tool geometry on cutting forces and tool wear when up-milling high-density fiberboard with alumina ceramic cutting tools, and found the tools with smaller rake angle can be used for high-speed cutting to improve tool life and productivity of processing. In order to verify the capability of PCD in finish milling of titanium alloys at a high feed rate, Ji et al. [21] investigated the surface roughness under different PCD tool geometries (radial rake angle, axial rake angle, and insert sharp radius), and found that its range is from 0.821 to 1.562 μm, which is suitable to titanium components. To reach a better machining quality and increased tool lifetime, Voss et al. [22] made a fundamental study in milling of unidirectional CFRP focusing on variable process parameters, tool geometries, and fiber orientations. A single-edged tool with cemented carbide inserts of variable macro geometry is utilized. Based on the excellent thermal conductivity of heat pipes, Uhlmann et al. [23] developed a milling cutter with a closed internal cooling system to improve heat dissipation of the cutting edge, and found that the cutting temperature was decreased and productivity was increased. Karpuschewski et al. [24] performed preliminary investigations to aid in the constructional design of the tool as well as the proper design of the seat of the inserts. The results of simulation can be utilized to increase the efficiency of face milling. It is well known that the indexable milling cutter consists of two parts: indexable inserts and cutter body. All the above literature could help optimize tool structure and improve cutting performance, and most of them focused on the geometric parameter optimization of solid-end mill and indexable insert. However, the research about the effect of cutter body geometry on cutting performance has rarely been reported.

In the cutting process, tool geometry has a direct impact on workpiece deformation, cutting forces, and tool wear, thereby

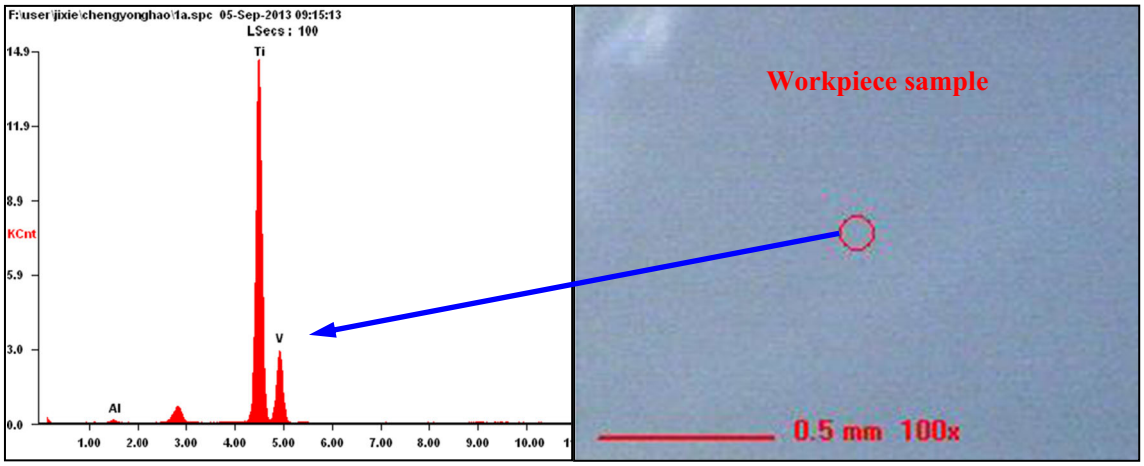

Element	Wt%	At%
AlK	07.34	12.35
TiK	88.36	83.81
V K	04.30	03.84

Fig. 1 The main chemical composition of the workpiece sample

affecting machinability, surface quality, and tool life. For indexable milling cutters, the tool geometry does not only refer to the geometric parameters of indexable insert but also includes the structural parameters of the cutter body, which determine the working angles and the inherent dynamic characteristics of cutters. Therefore, it is of great significance to make an in-depth study of the effect of cutter body geometry on the milling process.

Titanium alloy is one of the main structural materials in the aerospace field due to its superior performance such as high specific strength, fatigue resistance, corrosion resistance, and good heat resistance. However, it also falls into a typical difficult-to-machine material with the problems of low-thermal conductivity, high-chemical activity at elevated temperature, high-cutting force per unit area, and tool wear easily during machining, which seriously affect the surface integrity and fatigue properties of the machined components. Thus, high-performance machining of titanium alloy has become a major problem in modern manufacturing. In the present work, the performance of the same series of indexable face-milling cutters with different diameters was investigated during dry face milling of Ti-6Al-4V so as to improve the machinability of titanium alloy. Three-dimensional (3D) models of these indexable milling cutters were reconstructed and the corresponding dynamic characteristics were analyzed. The cutting performance of these cutters in terms of cutting forces, surface quality, and tool wear rate was investigated. This study will provide guidance for the design of indexable milling cutters for high-performance machining of titanium alloys.

2 Experimental details

2.1 Workpiece and cutting tools

The workpiece sample used in this study was a titanium alloy Ti-6Al-4V cuboid with the dimension of 170 mm × 85 mm × 80 mm. Its chemical composition was shown in Fig. 1, measured by EDAX vision spectrum. The sample density measured by electronic scale was about 4.44 g/cm^3, and the average surface hardness measured by digital micro-hardness tester HXS-1000AK was about 303.8 HV. In order to facilitate the installation of the dynamometer, four threaded holes with a

Table 1 Designation of the indexable milling cutters used in the experiments

Indexable insert	Cutter body	Diameter	Teeth	Sign
SPMT1204AEN WSP45	F2233.W.040.Z04.07	40 mm	4	Tool A
	F2233.B.080.Z06.07	80 mm	6	Tool B
	F2233.B.125.Z08.07	125 mm	8	Tool C

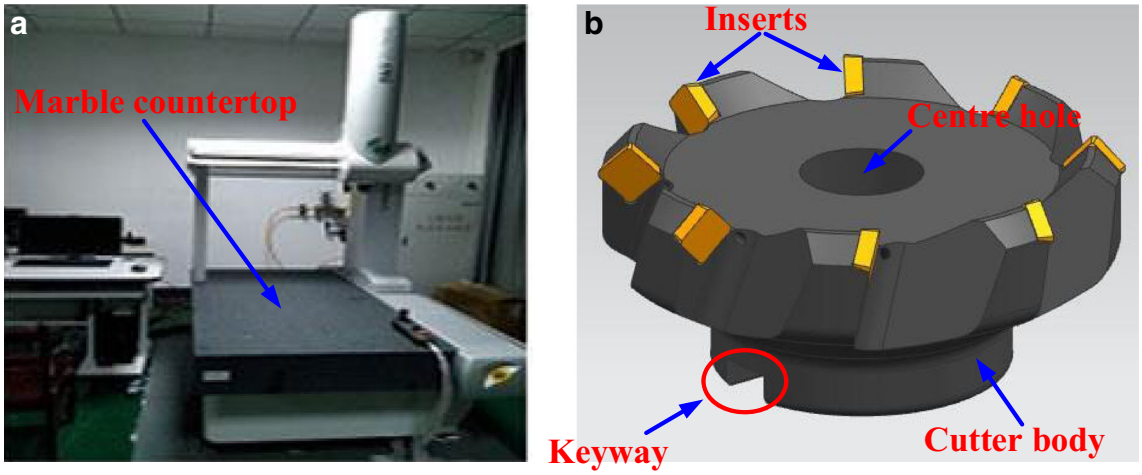

Fig. 2 Model reconstruction: **a** the measuring platform of CMM and **b** 3D reconstruction model of tool C

diameter of 8 mm and a depth of 16 mm were tapped at the bottom of the sample.

The cutting tools studied in this paper were the F2233 series of indexable face-milling cutters, produced by German Walter Group. Three kinds of cutter bodies with different diameters were equipped with the same type of indexable inserts for cutting performance tests. The specific details of these cutters were listed in Table 1.

2.2 Dynamic characteristic analysis

In order to obtain the dynamic characteristics of these cutters, the finite element method was adopted to reduce the expensive cost of the dynamic characteristic tests. In order to ensure the reliability of the calculation results, an accurate 3D geometric model of the cutter needs to be established. Coordinate-measuring machine (CMM) is a large-scale precision-measuring instrument that can accurately measure the geometric tolerance of a workpiece. It is often used for engineering tasks such as part detection, shape measurement, and process control. Therefore, in the present work, the contours of these cutters were measured using a global classic CMM with the designation of SR 07.10.07, produced by Hexagon, Sweden. Figure 2a shows the measuring platform of CMM.

Table 2 Material constants of the indexable milling cutters used in the experiments

Type	Elastic modulus	Poisson's ratio	Density
Cutter body	206 GPa	0.32155	7850 kg/m^3
Indexable insert	550 GPa	0.25	14,500 kg/m^3

In order to accurately reconstruct the cutter model, the key is to determine the relative position of the insert mounting surface on the cutter body. First, establish the tool coordinate system *Oxyz*: taking the marble countertop of the CMM as the reference plane *xy*, lay the cutter body flat with the keyway end facing down, and determine the position of the center axis *z* by the measuring probe based on the center hole of the cutter, and the origin *O* is the intersection of the *z*-axis and the *xy* plane. Subsequently, measure several points directly on each insert mounting surface. In this work, a bulb-ended probe with a diameter of 2 mm was used, and the measurement result was compensated before exported. Finally, import the exported data into a 3D-modeling software UGNX 8.5, and reconstruct the cutter model, referring to the description of the general catalog [25]. Figure 2b displays the 3D reconstruction model of tool C. In this figure, some minor features, such as the shape of the rake face and the bolts used to fix the inserts, are all neglected for ease of calculation.

In order to calculate the dynamic characteristics of these cutters, free modal analysis was carried out with the software version ANSYS 12.1. Before the calculation, some preprocessing needs to be done. At first, import the geometric model reconstructed above, and select the element type. In this work, the SOLID186 element was chosen due to its excellent properties such as high-order 3D solid structural unit with 20 nodes, quadratic displacement mode, and arbitrary spatial anisotropy. Then, set the material constants according to Table 2, and handle the junctions. Since there is no relative motion between indexable inserts and cutter body, which is consistent with the physical assumption of "GLUE," so the junctions between inserts and cutter body were handled by the "GLUE" operation. Hereafter, mesh the model and set the solution type and method. Here, free mesh with the tetrahedral element was used, and "Smartsize" tool was set at 6 to control

Table 3 The experimental scheme

Run no.	Cutting speed V_c (m/min)	Feed rate per tooth f_z (mm/z)	Cutting depth a_p (mm)	Cutting width a_e (mm)
1	65	0.15	1.5	15
2	65	0.2	0.5	20
3	40	0.15	1	20
4	90	0.2	1	15
5	40	0.2	1.5	25
6	40	0.1	0.5	15
7	90	0.15	0.5	25
8	65	0.1	1	25
9	90	0.1	1.5	20

the gridding size. Due to the fast speed, the block Lanczos method was used to extract the first 11 modes. Since no load or constraint is required, the first six orders of them are rigid body modes with a frequency of zero. Therefore, they are negligible in the free modal analysis. At last, solve the problem and view the results.

2.3 Cutting performance tests

The cutting performance tests were performed on the Mikron UCP800Duro CNC machining center. Cutters and workpiece used in the tests have been introduced before. In order to clarify the evolution of milling forces clearly, only two inserts were engaged in the milling process, and they were symmetrically mounted on the cutter body. The cutting performance of these cutters was assessed in terms of cutting forces, surface roughness, and tool wear rate. The cutting force signals were collected through a dynamometer Kistler 9257A, equipped with a charge amplifier Kistler 5070A, a data acquisition processing system Kistler 5697A, and a notebook with software DynoWare Kistler 2825A. The sampling rate was set at 1 kHz. Each run was milling along the length of the workpiece so as to guarantee the same cutting distance. After each run, the surface roughness of the workpiece was measured by a portable surface-roughness tester Mitutoyo 178–561-02A Surftest SJ-210, and the flank wear land width of each insert was evaluated by a Rational-WH video-measuring system VMS-1510G with software QIM1008. The tool wear rate was calculated as the ratio of the average flank wear land width to the cutting time.

According to the recommended range of cutting parameters by the manufacturer and the results of several preliminary tests considering the productivity of rough milling, the experimental scheme was designed based on the orthogonal test table $L_9(3^4)$, as shown in Table 3. All the tests were carried out in dry condition.

3 Results and discussion

3.1 Effect of cutter body geometry on dynamic characteristics

As described in Section 2.2, the dynamic characteristics of the cutters are characterized by the first 11 free modes due to the dominant role of low-frequency vibration [26]. In order to reduce the vibration during milling, the cutter is required to have a very good rigidity, which means that the higher the first few modal frequencies of the cutter, the better. Neglecting the first six rigid body modes, the free modes of these cutters were displayed in Fig. 3. It can be seen that the dynamic characteristics of different cutters vary greatly, albeit with a similar trend in modal frequencies. Of all cutters, tool B has the

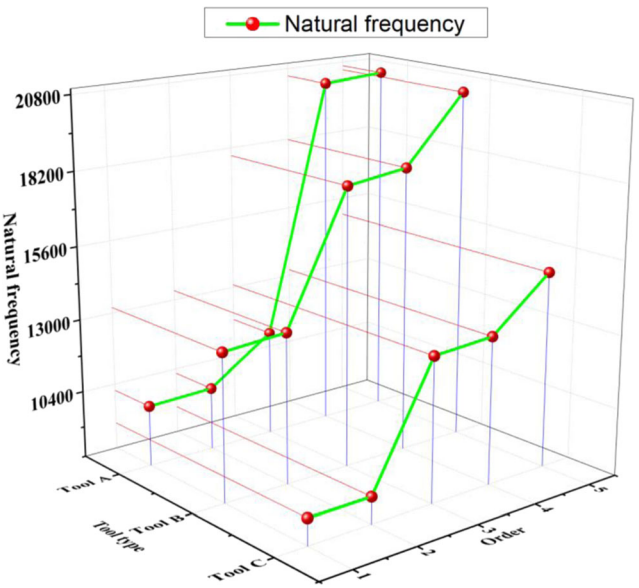

Fig. 3 The first five free modes of the cutters (neglecting rigid body modes)

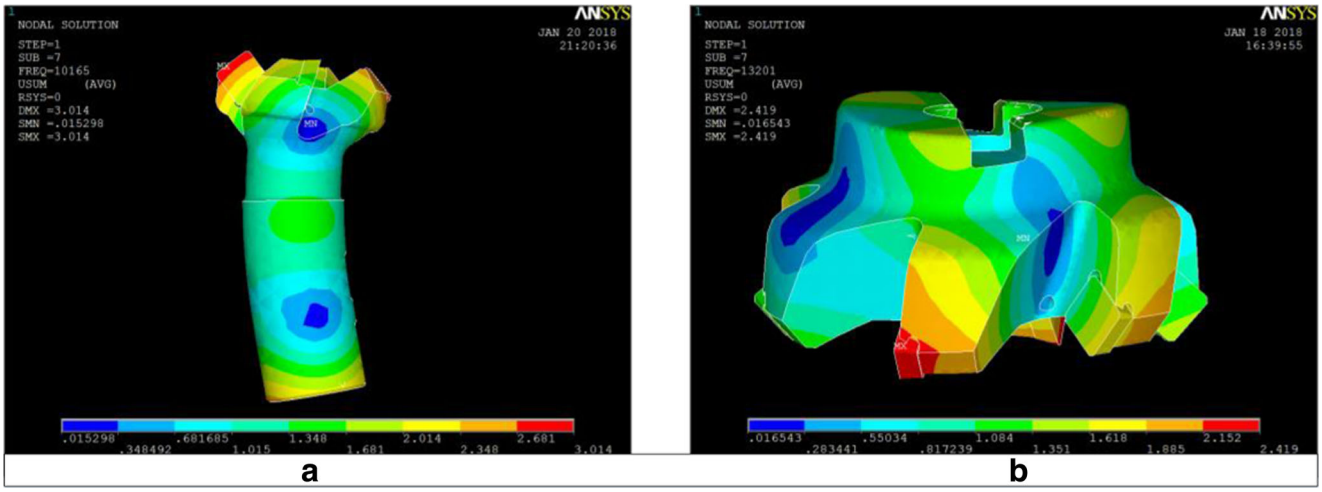

Fig. 4 First mode of **a** tool A and **b** tool B

highest first-order modal frequency, 13,201 Hz, which is 3035.9 Hz and 4262.2 Hz higher than tool A and tool C, respectively. This means tool B is the least susceptible to resonance and has the best rigidity. In this figure, two points with similar modal frequencies of the same cutter represent two symmetric modes. From this point of view, the 3rd, 4th, and 5th modes of tool A are significantly different from those of tool B and tool C, which can be attributed to the particular rod shape of tool A. For tool A, the 4th and 5th modes are symmetric modes, while for tool B and tool C, they appear in the 3rd and 4th modes. In addition, mode shape of the same order for different cutters is also very different. Taking the first mode as an example, tool A behaves as a bending mode in X direction, while tool B and tool C both show a torsion mode at the keyway end junction of the cutter body, as shown in Fig. 4.

3.2 Effect of cutter body geometry on cutting forces

Milling is an intermittent dynamic cutting process in which the cutting forces can be decomposed into static forces and dynamic forces [27]. The former mainly causes elastic deformation, while the latter leads to the forced vibration of machine tool-workpiece-cutter elastic system, and the resulting relative displacement will change the correct positional relationship between the cutter and the workpiece and leave the chatter marks on the machined surface, thereby reducing the precision and finish of the machined parts [28]. So, the characteristics of static and dynamic forces can reflect the cutting performance of the cutter to a certain extent.

In order to figure out the cutting force characteristics of different cutters, the spectral analysis was carried out on the cutting force signals acquired under the above experimental conditions. Figure 5 shows the spectral analysis results of the cutting force in the Z direction when the cutting was in the stable phase. The amplitude at the frequency of 0 Hz refers to the static force, which can characterize the elastic deformation, while the amplitude at other frequencies belongs to the dynamic force. It can be clearly observed that the dynamic force contains extremely rich frequency components, which have a common fundamental frequency, namely the cutting frequency of cutter teeth. Therefore, it can be considered that the vibration generated during the milling process is mainly forced vibration. The largest forced vibration occurs at the point of maximum amplitude, where the quality of the machined surface is the worst. Hence, these two indexes were extracted to reflect the cutting performance of the cutter.

Figure 6 illustrates the variation of static force and maximum dynamic force in the Z direction under different cutting conditions. The red dash lines of tool A between run no. 4 and run no. 6 in the figure are just a schematic for the sake of differentiation, which represents that the static force and the maximum dynamic force of tool A in run no. 5 are much bigger than those of tool B and tool C. It can be clearly observed that the static force and the maximum dynamic force of tool C are the smallest under different cutting conditions, which means that tool C performs the best in this respect, while in most cases, tool A has the worst performance. Even in run no. 5 with cutting parameters $V_c = 40$ m/min, $f_z = 0.2$ mm/z, $a_p = 1.5$ mm, and $a_e = 25$ mm, the milling process of tool A was terminated due to the serious sticking phenomenon. The presence of built-up edge (BUE) led to the increase of cutting depth [29], making the cutting process more difficult. Furthermore, in the range of cutting parameters studied, the maximum difference of static force between different cutters reaches 203 N (happened in run no. 1), while that of dynamic cutting force is also up to 80 N (happened in run no. 3). This result shows that the cutter body geometry has a significant impact on cutting forces.

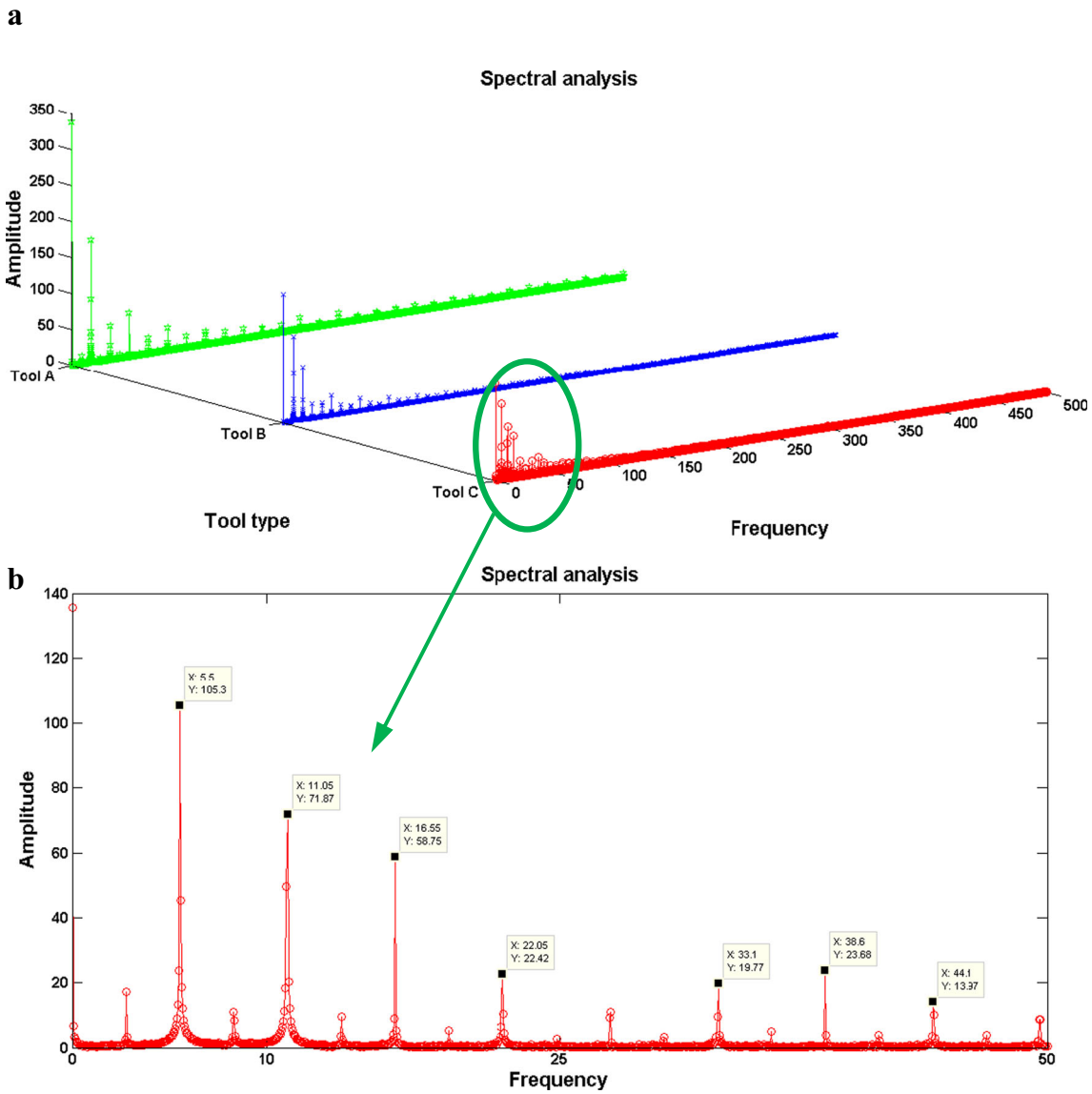

Fig. 5 Spectral analysis of the cutting force in the *Z* direction

3.3 Effect of cutter body geometry on surface quality

Surface quality has a significant impact on the performance of the parts and the reliability of the machine, which draws more and more attention. Generally, surface quality can be evaluated by indicators such as surface roughness, degree of work hardening of surface layer and depth of the hardened layer, the property and size of surface residual stress [2]. In the present work, only surface roughness was used to characterize the surface quality due to the limitation of experimental conditions.

After each run, the surface roughness at more than five random points on the machined surface was measured. Figure 7 shows the average surface roughness values under different cutting conditions. The meaning of red dash lines in the figure is the same with that in Fig. 6. As can be seen, under most of the cutting conditions, the quality of the machined surface formed by these cutters was very good, with the surface roughness varying between 0.3 μm and 0.7 μm. The possible reason for this result is the existence of the wiper on the indexable insert. Only the surface roughness of tool A shows abnormalities under run no. 4 and run no. 5, which can be attributed to the vibration caused by the change of the cutting depth and the formation and abscission of BUE. From the overall situation, the machined surface quality of tool B and tool C is better, which is in accordance with the variation of static force and maximum dynamic force in the *Z* direction in Fig. 6.

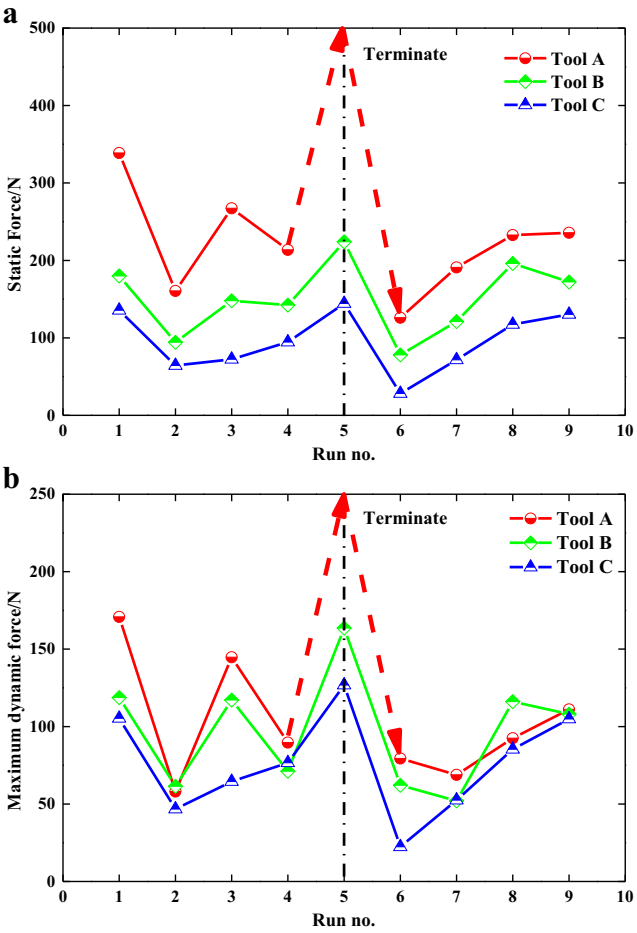

Fig. 6 Cutting force in the *Z* direction of different cutters: **a** Static force and **b** maximum dynamic force

3.4 Effect of cutter body geometry on tool wear

During the milling process, indexable inserts will be worn or partially damaged while cutting down the chips. However, worn inserts will reduce machining accuracy, increase surface roughness, lead to increasing cutting forces and cutting temperature, and even aggravate vibration. Therefore, the wear degree of inserts under the same cutting conditions can fully reflect the cutting performance of the cutter. In this paper, both major flank wear rate and minor flank wear rate were proposed as the indexes for estimating the wear degree of inserts because the wiper was also engaged in the face-milling process. A schematic diagram of the measured flank wear bandwidth is shown in Fig. 8. VB and WVB denote the wear bandwidth on the major and minor flank face, respectively.

Figure 9 shows the tool wear rates on major and minor flank face under different cutting conditions. It can be clearly observed that the variation trends of wear rate of different cutters with cutting conditions are the same, but the amplitude of variation is quite different. The maximum difference of the major flank wear rate between different cutters reaches 0.723 mm/min, while that of the minor flank wear rate is also up to 0.249 mm/min. They appear in runs no. 4 and no. 5, respectively. After these two runs, brittleness breakage was observed on all the inserts of tool A, as shown in Fig. 10.

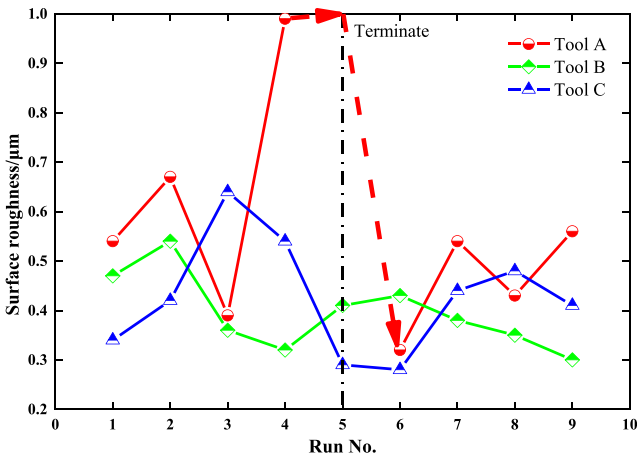

Fig. 7 The average surface roughness under different cutting conditions

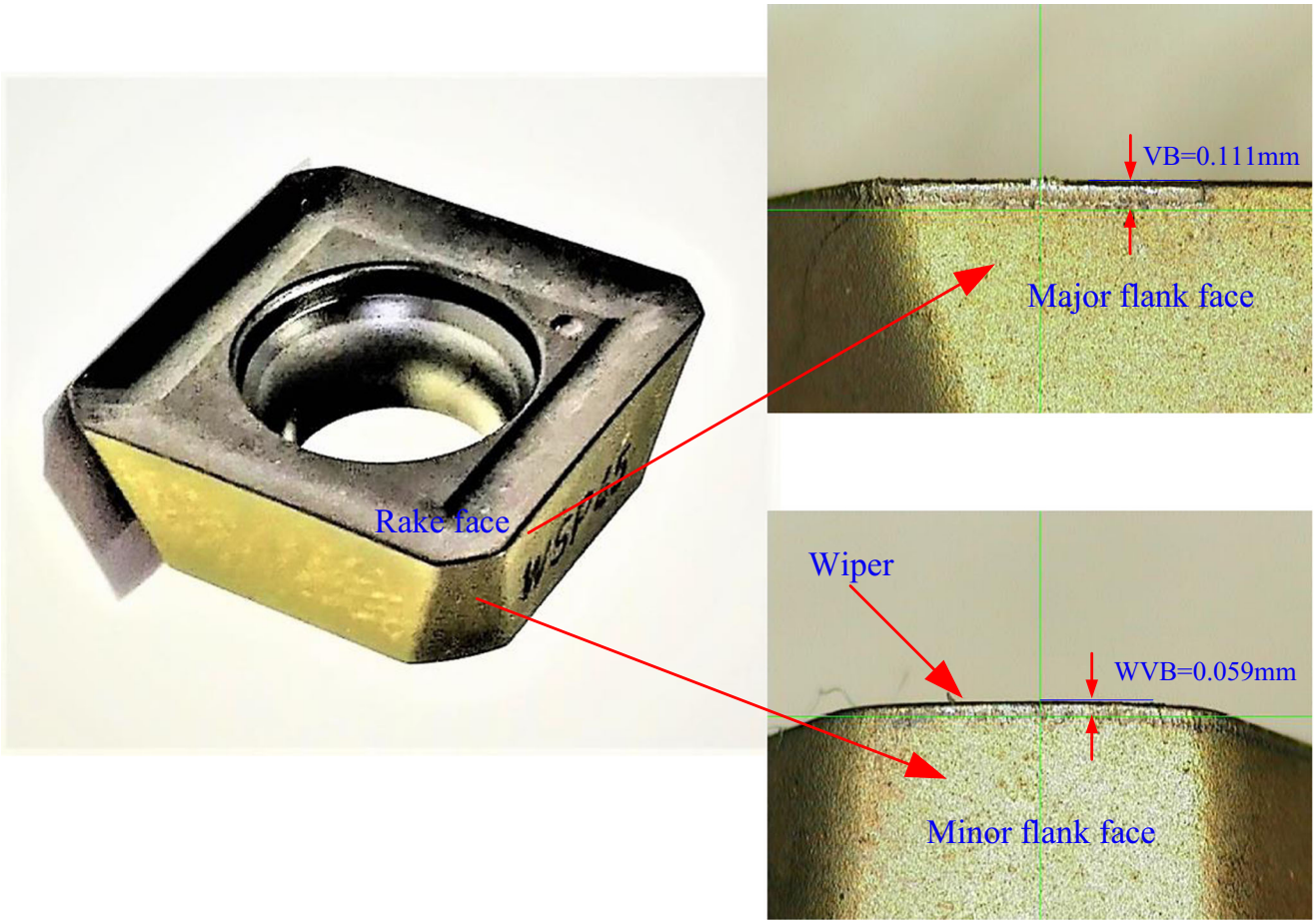

Fig. 8 Tool wear on major and minor flank face of tool C after run no. 3

This phenomenon can be attributed to intermittent impact loads and violent vibrations. In addition, of the three cutters, both the major flank wear rate and the minor flank wear rate of tool A show the highest value under all cutting conditions, while those of tool C behave the smallest, which means that tool C has the best wear resistance. This result is completely consistent with the trends of static force and maximum dynamic force in the Z direction in Fig. 6. It can be inferred that tool wear rate is highly correlated with static force and maximum dynamic force in the Z direction, especially for the minor flank wear rate. Therefore, the cutter body geometry has a significant effect on the wear resistance of the cutter.

3.5 Geometric structure analysis

In order to find out the reason why the cutting performance of the same series of milling cutters with different diameters has a big difference, an in-depth study of the geometric structure of the above milling cutters was carried out in this paper.

The indexable milling cutter is composed of a rotary milling cutter body and a number of indexable inserts. As discussed before, the outline dimensions of the cutter body determine the dynamic characteristics of the cutter. However, according to the data measured by CMM, apart from the outline dimensions of the cutter body, there are still two key parameters, namely the center offset and the installation angle of the insert, which determine the geometric structure of the cutter, as shown in Fig. 11. In the figure, the Z axis is the center axis of the cutter, while the XOY plane represents the bottom surface of the cutter; the center offset e of the insert denotes the distance between the origin O and the straight line AB which is the intersection between the plane where the rake face of the insert lies and the XOY plane, while the installation angle α of the insert refers to the included angle between the bottom of the insert and the Z axis; D_c and a_e represent the cutting diameter and the cutting width, respectively. Based on the measured data, the center offset and the installation angle were calculated, as shown in Table 4. It can be seen that with the increase of cutting diameter, the center offset

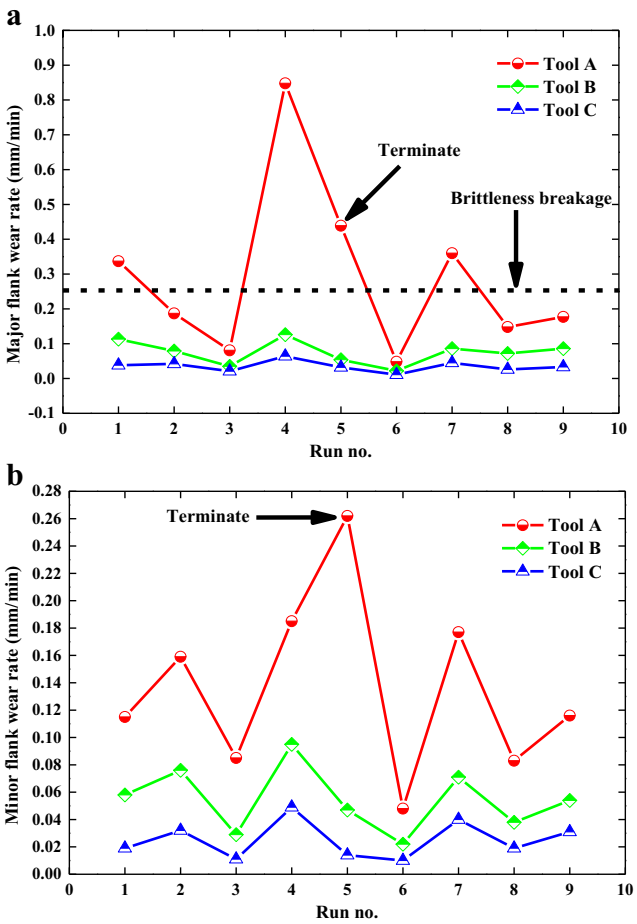

Fig. 9 Tool wear rates on **a** major flank face and **b** minor flank face under different cutting conditions

gradually increases, while the installation angle gradually decreases. The different combination of center offset and installation angle not only affects the dynamic characteristics of the cutter but also determines the working angle of the cutter. These parameters, together with the outline dimensions of the cutter body, jointly determine the cutting performance of the cutter.

4 Conclusions and future work

In this paper, the performance of the same series of indexable milling cutters with different diameters was investigated. The dynamic characteristics and cutting performance of these cutters were analyzed. The following conclusions are drawn:

(1) Of all cutters, tool B is the least susceptible to resonance with the highest first-order modal frequency of 13,201 Hz. Mode shape of the same order for different cutters is very different.

(2) Tool C performs the best in terms of static force and maximum dynamic force.

(3) The machined surface quality was very good with the surface roughness varying between 0.3 μm and 0.7 μm due to the existence of the wiper. The abnormalities in the surface roughness of tool A can be attributed to the vibration caused by the change of the cutting depth and the formation and abscission of BUE.

(4) Tool C has the best wear resistance, and tool wear rate is highly correlated with static force and maximum dynamic force in the Z direction, especially for the minor flank wear rate.

(5) The different combination of center offset and installation angle, together with the outline dimensions of the cutter body, jointly determines the cutting performance of the cutter.

Future work will focus on the investigation on the mechanism of center offset and installation angle and the design optimization of a certain type of indexable milling cutter.

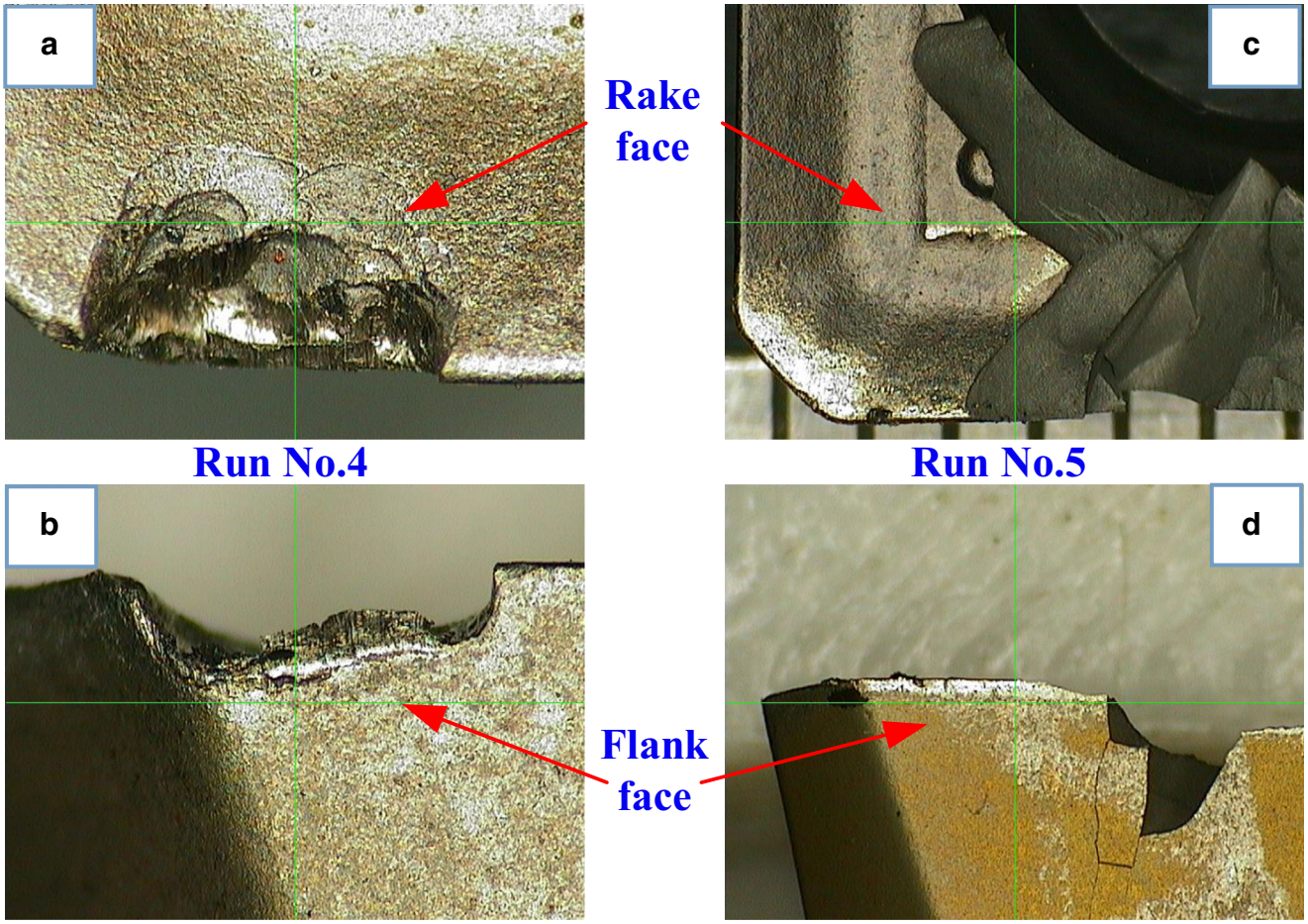

Fig. 10 Brittleness breakage of tool A: **a** rake face and **b** flank face after run no. 4; **c** rake face and **d** flank face after run no. 5

Acknowledgements The authors are very grateful to the experimental platform provided by the advanced manufacturing and technology experiment center.

Funding information This research is financially supported by the National Science and Technology Major Project of China (grant no. 2012ZX04003-021).

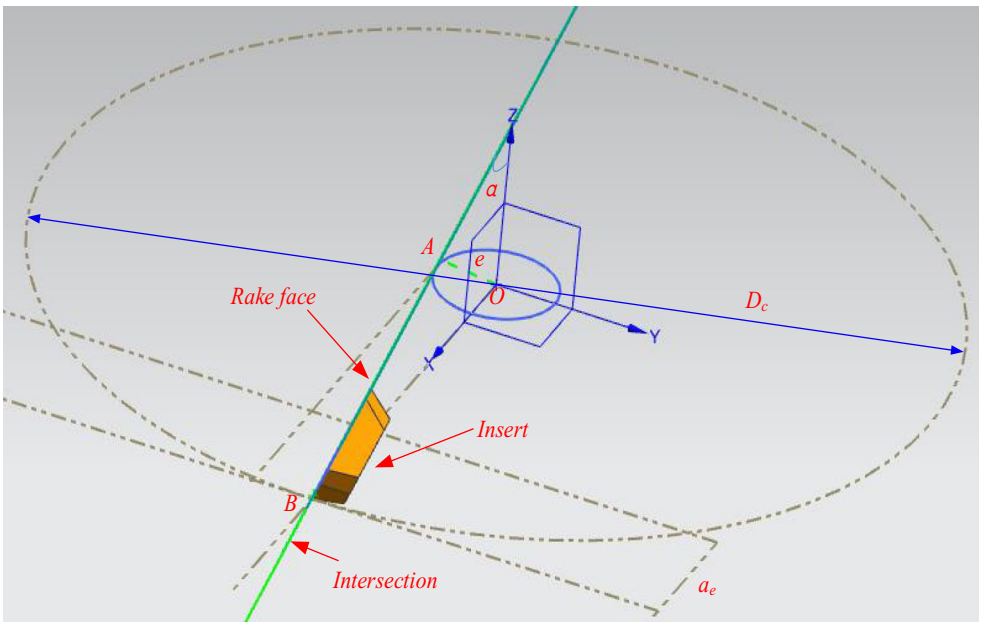

Fig. 11 Definition of center offset and installation angle of the insert

Table 4 The center offset e and the installation angle α of the insert for the three cutters

Type	Cutting diameter D_c/mm	Center offset e/mm	Installation angle α/°
Tool A	40	3.7429	10.7906
Tool B	80	7.6019	10.6546
Tool C	125	12.2081	10.6049

References

1. Ng EG, Szablewski D, Dumitrescu M, Elbestawi MA, Sokolowski JH (2004) High speed face milling of a aluminium silicon alloy casting. CIRP Ann Manuf Technol 53(1):69–72. https://doi.org/10.1016/S0007-8506(07)60647-7
2. Chen RY (2002) Principle of metal cutting. China Machine Press, Beijing
3. Yan X (2000) Research on the theory and methods of free-cutting tools design with applications. Dissertation, Huazhong University of Science and Technology
4. Liu ZQ (2006) Advanced tool design technology: tool structure, tool materials and coating technology. Aeronaut Manuf Technol 07:38–42. https://doi.org/10.3969/j.issn.1671-833X.2006.07.002
5. Han CL, Den CH, Zhao DF, Hu KH (2012) Milling performance of TiC-Ni cermet tools toughened by TiN nanoparticles. Int J Refract Met Hard Mater 30(1):12–15. https://doi.org/10.1016/j.ijrmhm.2011.06.005
6. Kim J, Kim M, Kang M, Kang S (2013) Material properties and tool performance of Ti-based solid solution cermets for micro end-mill applications. Int J Refract Met Hard Mater 36:278–282. https://doi.org/10.1016/j.ijrmhm.2012.10.005
7. Su HH, Liu P, Fu YC, Xu JH (2012) Tool life and surface integrity in high-speed milling of titanium alloy TA15 with PCD/PCBN tools. Chin J Aeronaut 25(5):784–790. https://doi.org/10.1016/S1000-9361(11)60445-7
8. Ogawa Y, Ota M, Nakamoto K, Fukaya T, Russell M, Zohdi TI, Yamazaki K, Aoyama H (2016) A study on machining of binder-less polycrystalline diamond by femtosecond pulsed laser for fabrication of micro milling tools. CIRP Ann Manuf Technol 65(1):245–248. https://doi.org/10.1016/j.cirp.2016.04.081
9. Lu L, Wang QM, Chen BZ, Ao YC, Yu DH, Wang CY, Wu SH, Kim KH (2014) Microstructure and cutting performance of CrTiAlN coating for high-speed dry milling. Trans Nonferrous Metals Soc China 24(6):1800–1806. https://doi.org/10.1016/S1003-6326(14)63256-8
10. Hei HJ, Ma J, Li XJ, Yu SW, Tang B, Shen YY, Tang WZ (2015) Preparation and performance of chemical vapor deposition diamond coatings synthesized onto the cemented carbide micro-end mills with a SiC interlayer. Surf Coat Technol 261:272–277. https://doi.org/10.1016/j.surfcoat.2014.11.019
11. Skordaris G, Bouzakis KD, Kotsanis T, Charalampous P, Bouzakis E, Lemmer O, Bolz S (2016) Film thickness effect on mechanical properties and milling performance of nano-structured multilayer PVD coated tools. Surf Coat Technol 307(A):452–460. https://doi.org/10.1016/j.surfcoat.2016.09.026
12. Aslantas K, Hopa HE, Percin M, Ucun İ, Çicek A (2016) Cutting performance of nano-crystalline diamond (NCD) coating in micro-milling of Ti_6Al_4V alloy. Precis Eng 45:55–66. https://doi.org/10.1016/j.precisioneng.2016.01.009
13. Liu W, Li AQ, Wu HD, Long Y, Huang JW, Deng X, Wang CY, Wang QM, Wu SH (2016) Effects of gas pressure on microstructure and performance of (Ti, Al, Zr)N coatings produced by physical vapor deposition. Ceram Int 42(15):17436–17441. https://doi.org/10.1016/j.ceramint.2016.08.045
14. Liu W, Chu QQ, Zeng JJ, He RX, Wu HD, Wu ZW, Wu SH (2017) PVD-CrAlN and TiAlN coated Si_3N_4 ceramic cutting inserts-2. High speed face milling performance and wear mechanism study. Ceram Int 43(12):9488–9492. https://doi.org/10.1016/j.ceramint.2017.04.127
15. Saptaji K, Subbiah S, Dhupia JS (2012) Effect of side edge angle and effective rake angle on top burrs in micro-milling. Precis Eng 36(3):444–450. https://doi.org/10.1016/j.precisioneng.2012.01.008
16. Subramanian M, Sakthivel M, Sooryaprakash K, Sudhakaran R (2013) Optimization of end mill tool geometry parameters for Al7075-T6 machining operations based on vibration amplitude by response surface methodology. Measurement 46(10):4005–4022. https://doi.org/10.1016/j.measurement.2013.08.015
17. Ji CH, Liu ZQ, Ai X (2014) Effect of cutter geometric configuration on aerodynamic noise generation in face milling cutters. Appl Acoust 75:43–51. https://doi.org/10.1016/j.apacoust.2013.07.004
18. Huang PL, Li JF, Sun J, Zhou J (2014) Study on performance in dry milling aeronautical titanium alloy thin-wall components with two types of tools. J Clean Prod 67:258–264. https://doi.org/10.1016/j.jclepro.2013.12.006
19. Warhanek M, Pfaff J, Martin P, Schönbächler L, Boos J, Wegener K (2016) Geometry optimization of polycrystalline diamond tools for the milling of sintered ZrO_2. Procedia CIRP 46:290–293. https://doi.org/10.1016/j.procir.2016.04.003
20. Zhu ZL, Guo XL, Ekevad M, Cao PX, Na B, Zhu NF (2017) The effects of cutting parameters and tool geometry on cutting forces and tool wear in milling high-density fiberboard with ceramic cutting tools. Int J Adv Manuf Technol 91(9–12):4033–4041. https://doi.org/10.1007/s00170-017-0085-8
21. Ji W, Liu XL, Wang LH, Sun SL (2015) Experimental evaluation of polycrystalline diamond (PCD) tool geometries at high feed rate in milling of titanium alloy TC11. Int J Adv Manuf Technol 77(9–12):1549–1555. https://doi.org/10.1007/s00170-014-6517-9
22. Voss R, Seeholzer L, Kuster F, Wegener K (2016) Influence of fibre orientation, tool geometry and process parameters on surface quality in milling of CFRP. CIRP J Manuf Sci Technol 18:75–91. https://doi.org/10.1016/j.cirpj.2016.10.002
23. Uhlmann E, Riemer H, Schröter D, Sammler F, Richarz S (2017) Substitution of coolant by using a closed internally cooled milling tool. Procedia CIRP 61:553–557. https://doi.org/10.1016/j.procir.2016.11.267
24. Karpuschewski B, Kundrák J, Felhő C, Varga G, Sztankovics I, Makkai T, Borysenko D (2018) Preliminary investigations for the effect of cutting tool edge geometry in high-feed face milling. Vehicle Auto Eng 241–254. https://doi.org/10.1007/978-3-319-75677-6_20
25. (2012) Walter, General catalogue_ A compendium of expertise in machining
26. Tobias SA (1977) Machine-tool vibration. China Machine Press, Beijing
27. Li JZ (1993) Metal cutting dynamics. Zhejiang University Press, Zhejiang
28. Yang S, Tang HL, Liao BY (1983) Machine tool dynamics. China Machine Press, Beijing
29. Xiong LS, Yan XG, Zhang FR (2006) Fundamentals of mechanical manufacturing technology, 3rd edn. Huazhong University of Science and Technology Press, Wuhan